Opto-electrochemical spectroscopy of *trans*-$(CH)_x$

A. Feldblum, J. H. Kaufman, S. Etemad, and A. J. Heeger
Department of Physics, University of Pennsylvania, Philadelphia, Pennsylvania 19104-3859

T. -C. Chung and A. G. MacDiarmid
Department of Chemistry, University of Pennsylvania, Philadelphia, Pennsylvania 19104-3895
(Received 23 February 1982)

Detailed quantitative studies of the visible near-ir absorption spectra of *trans*-$(CH)_x$ have been carried out in the semiconducting, transitional, and metallic regimes. With the use of the opto-electrochemical technique to take advantage of the control and precision of electrochemical doping, the absorption data were obtained *in situ*, during the doping process. Thin $(CH)_x$ films were polymerized on conducting glass and used as one electrode in an electrochemical cell ($Li^+ClO_4^-$ in propylene carbonate) with a strip of Li metal as the counter electrode. As the *trans*-$(CH)_x$ was doped from $y < 0.003$ to $y \simeq 0.08$, the interband absorption peak decreased and the midgap absorption increased in intensity. The quantitative agreement with the calculations of the soliton model and the universal nature of the data provide direct evidence for the existence of charged solitons in doped *trans*-$(CH)_x$. The results show that in the concentration range $2\times10^{-3} < y < 5\times10^{-2}$, where independent experiments have established that the high conductivity is due to spinless carriers, the semiconductor gap persists with little change in magnitude. Moreover, the absorption data identify these carriers as charged solitons. Kinetic studies following a step change in applied cell voltage indicate a time constant for the approach to equilibrium (after an initial faster transient) in the range from 6 to 10 h. This long time constant results from diffusion of the dopant ions within the $(CH)_x$ fibrils. Analysis of the approach to equilibrium and direct analysis of the spectra at intermediate doping levels demonstrate that phase separation with the formation of metallic "particles" does not occur. Hysteresis in the intensity of the midgap transition as a function of applied voltage has been interpreted as a direct indication of single-charge injection via polarons which subsequently combine to form lower-energy soliton pairs.

I. INTRODUCTION

Direct evidence for the existence of charged solitons in *trans*-$(CH)_x$ at dilute doping levels comes from optical absorption measurements.[1] Within the soliton model there is a localized electronic state associated with each solition.[2–6] Because of the electron-hole symmetry appropriate to polyacetylene (one π electron per carbon atom), the energy of this localized state is precisely at midgap. Although the Coulomb potential of the dopant molecule and electron-electron interactions may shift this energy, the large size of the soliton implies that such shifts will be relatively small. Moreover, they are in opposite directions. As a result of electron-electron repulsion, the configuration with a localized spin in the midgap state has a lower energy than that of the charged soliton. Thus the effect of electron-electron repulsion is to reduce the net transition energy; whereas the binding of the charged soliton to the nearby ion will raise the energy. Consequently these two tend to cancel. As a result, a midgap peak is expected to appear in the optical absorption spectrum upon doping, with an intensity proportional to the concentration of dopant molecules, but with a shape and position (in energy) which is insensitive to the dopant type.

Suzuki *et al.*[1] presented the first experimental evidence of the midgap absorption using AsF_5 doping at dilute levels. Since then, the generality of the midgap absorption has been verified using a variety of acceptors (p type) and donors (n type).[7,8] Suzuki *et al.*,[1] furthermore, attempted a quantitative comparison of the strength of the midgap transition (and the related decrease in the interband transition) to the predictions as calculated from the

soliton wave functions. However, a detailed quantitative analysis of the experimental results in comparison with theory has not yet been carried out for two reasons. Firstly, the vapor-phase-doping technique utilized in earlier experiments was difficult to control. Particularly at dilute concentrations and for thin films on substrates (where weight uptake methods are not appropriate), the precise dopant levels are uncertain. Moreover, the short doping periods required for such low levels of vapor-phase doping leaves open the question of dopant uniformity. Secondly, because of the subtlety of the electronic wave functions (both band states and localized soliton state) appropriate to a *trans*-$(CH)_x$ chain containing a soliton, the theoretical predictions have been the subject of considerable discussion in the literature.[9–11] The two relevant transitions (midgap and interband) for a *trans*-$(CH)_x$ chain containing a soliton are indicated on Fig. 1.

Suzuki *et al.*[1] calculated the strength and (ideal) line shape of the midgap transition for a one-dimensional (1D) model

$$\alpha_s(\omega)=A(\pi^2\xi/a)f_s(\omega)\ , \tag{1a}$$

$$f_s(\omega)=\frac{E_g/2}{[(\hbar\omega)^2-(E_g/2)^2]^{1/2}} \times \operatorname{sech}^2\frac{\pi}{2}\left[\frac{[(\hbar\omega)^2-(E_g/2)^2]^{1/2}}{E_g/2}\right], \tag{1b}$$

where $A\equiv 16\pi\hbar e^2\,|\,M_x\,|^2/m^2ncWE_g$, $E_g\equiv 2\Delta_0$ is the 1D energy gap, W is the full bandwidth ($\sim 10-12$ eV), m and e are the electron mass and charge, c is the velocity of light, and n is the index of refraction. The factor $(\pi^2\xi/a)$ indicates an enhancement of the soliton transition resulting directly from the extended spatial delocalization of the soliton wave function ($\xi/a \gg 1$ is the half-width of the kink in units of the C-C lattice constant). For $W=10$ eV and $E_g=1.4$ eV, one finds $\xi\simeq 7a$ so that $(\pi^2\xi/a)\simeq 70$. As a result, the transitions involving the soliton level should be observable even at extremely small concentrations. This transition has been reexamined in several papers[9–11]; Eq. (1) is the correct result.

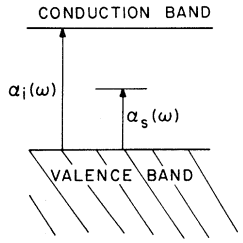

FIG. 1. Schematic diagram showing the interband and midgap transitions.

The interband transition $\alpha_i(\omega)$ per carbon atom, in the presence of a kink is correspondingly decreased and the total oscillator strength is conserved. The result is

$$\alpha_i(\omega)=\alpha_0(\omega)(1-y\,2\xi/a) \tag{2}$$

to lowest order in the soliton concentration y where $\alpha_0(\omega)$ describes the interband transition for a perfect chain (i.e., with no solitons):

$$\alpha_0=Af_0(\omega)\ , \tag{3a}$$

$$f_0(\omega)=\left[\frac{E_g}{\hbar\omega}\right]^2\Bigg/\left[\left[\frac{\hbar\omega}{E_g}\right]^2-1\right]^{1/2}. \tag{3b}$$

The interband transition for a chain containing a soliton was described incorrectly by Suzuki *et al.*[1] in their original paper and was corrected[12] later (in collaboration with Gammel and Krumhansl). A number of calculations of $\alpha_i(\omega)$ have appeared. The most comprehensive analysis was carried out by Kivelson *et al.*[10] who considered both the discrete lattice case of Su, Schrieffer, and Heeger (SSH)[2,3] and the continuum model of Takayama, Lin-Liu, and Maki (TLM).[5] Kivelson *et al.*[10] find that the uniform suppression implied by Eq. (2) is not exact, but is nevertheless an excellent approximation in the frequency range $\hbar\omega > 2.4\Delta$ [above about 1.9 eV for *trans*-$(CH)_x$]; i.e., the frequency range of importance in experimental studies of the interband transition.

The discovery of electrochemical doping[13–15] has resulted in the ability to dope polyacetylene *p* type or *n* type with control of the dopant concentration. Since the level of doping, $[CH(ClO_4)_y]_x$, is determined by the voltage across the cell, a desired dopant concentration can be established by using the independently measured V vs Q curve. Moreover, by allowing the cell to come to equilibrium at a given voltage, optimum dopant uniformity can be achieved. Therefore, the use of electrochemical doping makes possible, for the first time, a quantitative comparison of the experimental results with theoretical predictions.

In this paper, we present a quantitative, *in situ* study of the absorption spectrum during the electrochemical doping process and as a function of the dopant concentration for $[CH(ClO_4)_y]_x$. The

strength of the midgap transition is in quantitative agreement with theory. As the *trans*- $(CH)_x$ was doped from $y < 0.003$ to $y > 0.08$ the midgap absorption peak increased, and the interband absorption peak decreased in intensity. The spectra demonstrate that the midgap oscillator strength comes from the interband transition over a broad frequency range above 1.6 eV, consistent with the uniform suppression indicated in Eq. (2). These spectral features, i.e., the midgap and the interband absorptions, persist throughout the transitional regime. Only at the highest levels, $y > 0.07$, are the data characteristic of the free-carrier absorption expected for a metal. The question of inhomogeneous doping and metallic "particle" formation is addressed. From studies of the approach to equilibrium and from direct analysis of the spectra at intermediate doping levels, it is shown that phase separation, with the formation of metallic "particles" does not occur. Hysteresis in the intensity of the midgap transition as a function of applied voltage has been interpreted in terms of single-charge injection via polarons which subsequently combine to form lower energy charged soliton pairs. Charge removal (on discharge) then takes place from the midgap levels. The experimental techniques are described in Sec. II, and the data are presented in Sec. III. The results are discussed and compared with theory in Sec. IV.

II. EXPERIMENTAL TECHNIQUES

Electrochemical doping of polyacetylene (either *p* type or *n* type) can be accomplised by using a $(CH)_x$ film as an electrode in an electrochemical cell.[13–15] The experiments reported here utilized *trans*-$(CH)_x$ versus lithium metal with the electrolyte being $1M$ $Li^+ClO_4^-$ in propylene carbonate. Independent studies have shown that neutral $(CH)_x$ is about 2.2—2.6 V positive relative to lithium, and that a threshold voltage of about 3.0 V exists for charge injection during the doping process. Thus, to dope the polymer *p* type, a voltage in excess of 3.0 V is applied across the cell. Resetting the voltage back to ~2.5 V returns the $(CH)_x$ film to the neutral state. Similarly, to dope the film *n* type, the voltage is reduced to values below 2 V.

The electrochemical doping procedure has two advantages over chemical doping. The first (mentioned above) is the control over the dopant level made possible through electrochemical doping. Using a stabilized constant voltage source with a millivolt setting accuracy, any desired dopant level can be achieved by setting a specific voltage across the cell and waiting for attainment of diffusion-controlled equilibrium (or near equilibrium) of the dopant ions throughout the $(CH)_x$ fibrils (the kinetics of the approach to equilibrium are described in Sec. III B). For example, to dope the film to about 5%, $[CH(ClO_4)_{0.05}]_x$, the applied voltage (which will be essentially identical to the cell voltage under near-equilibrium conditions) should be about 3.7 V. The V vs Q curve for a known weight of free standing (~0.1-mm-thick) *trans*-$(CH)_x$ film has been generated[16] by electrochemically doping the film in a $1M$ solution of $LiClO_4$ in propylene carbonate, and then allowing it to stand for one day to permit diffusion of the ClO_4 ions from the surface to the interior of the $(CH)_x$ fibrils. The potential of the doped $(CH)_x$ film (vs Li) is then recorded and the charge liberated, as the doped film is electrochemically returned to a voltage of 2.5 V [characteristic of neutral $(CH)_x$], is measured. From the charge liberated and the weight of the film employed, the level of doping corresponding to the quasiequilibrium potential is calculated. Repetition of this procedure at different levels of doping gives the V vs Q curve. In the present experiments, doping levels were achieved by applying a fixed voltage and allowing the system to come to equilibrium. Since each dopant ion carries unit charge, knowledge of V vs Q is equivalent to knowledge of V vs y.

A second advantage of electrochemical doping is that it allows for a "clean" undoping procedure with the same precision as the doping half of the cycle. Unlike chemical compensation no salts are formed, so that the pristine neutral film can be measured after the doping-undoping cycle.

In order to be able to carry out optical measurements on the film during the electrochemical doping process, a special cell was constructed. The lithium metal strip and the $(CH)_x$ were in two arms of the cell, joined at the bottom. Part of the bottom of the cell was filled with active alumina; the electrolytic solution extended into both arms completing the internal circuit. The arms of the cell which contained the $(CH)_x$ film were constructed of rectangular tubing (9-mm×3-mm i.d.) in order to minimize scattered light, to prevent divergence of the beam, and to minimize the ratio of electrolyte to $(CH)_x$ volumes.

The thin $(CH)_x$ film was polymerized during approximately 5 sec using experimental techniques similar to those developed by Shirakawa and colleagues,[17] but modified so as to obtain uniform

thin films on a glass substrate.[18] In order to make electrical contact, the substrate used was conducting glass. The upper edge of the rectangular glass substrate was kept free of $(CH)_x$ and was notched so that a wire could be wrapped around it to make a good pressure contact to the conducting surface. To maintain long-term stability of the cell, both arms were carefully sealed, with the wire contacts extending through the seals. The same cell containing the conducting glass, electrolyte, etc., but with no $(CH)_x$ film was used as a reference for determining the absorption background.

The absorption measurements were made utilizing a McPherson EU700 series monochrometer and an IR Industries Si-PbS two-color detector using standard light-chopping and lock-in amplifier techniques. The monochrometer and lock-in were interfaced to an Analog Devices MacSym II minicomputer for data acquisition and analysis. In a typical experiment, the reference cell was run first to obtain an effective "source" spectrum I_0 involving all absorptions not due to the $(CH)_x$. The data were stored in the MacSym II. The cell containing the $(CH)_x$ electrode was then rigidly mounted in the light path so that a single area was in the beam throughout the doping-undoping cycle, thus allowing quantitative *in situ* comparison of the spectra for each voltage (i.e., each dopant concentration). The raw transmission data I_t as well as the optical density $(-\ln I_t/I_0)$ were stored in the computer for each value of the applied voltage. The voltage across the cell was then changed to the next desired value, and the cell was allowed to come to equilibrium. During this time, the monochrometer was set at 0.8 eV, and the strength of the midgap transition, $\alpha_s(\omega)$, was monitored by the computer along with the cell current. Initially, after stepping the external voltage, current flows and then decays steadily with time as the cell approaches equilibrium. Typical currect levels were 500 nA after a voltage step falling to about 20 nA as the cell approaches diffusion equilibrium. At the same time, the absorption coefficient at 0.8 eV changes continuously and approaches a steady value characteristic of the new dopant concentration. After these parameters had reached steady state, a spectrum was taken. The data were analyzed in terms of the optical density or absorption coefficient,

$$\alpha = -(1/t)\ln I_t/I_0 ,$$

where the film thickness t was obtained from the optical density of the undoped *trans*-$(CH)_x$.

In situ optical studies during electrochemical doping have recently shown that doping *cis*-polyacetylene to a fixed dilute concentration induces partial *cis-trans* isomerization.[19] "Undoping" back to neutral $(CH)_x$ converts that portion of the sample which was doped back into undoped *trans*-$(CH)_x$. Subsequent doping to the same level (or to lower levels) redopes only that portion which is already *trans*. Although doping to a higher level induces additional isomerization, complete isomerization is not achieved until dopant levels are characteristic of the metallic state. The optical absorption results obtained during electrochemical isomerization are consistent with ^{13}C NMR data[20] which show major inhomogeneity for *cis*-$(CH)_x$ samples doped to intermediate levels but more nearly uniform doping in *trans*-$(CH)_x$. Therefore, since the dopant uniformity in *cis*-rich samples is determined by the history of partial isomerization and by the simultaneous isomerization induced during doping, the present study is restricted to doped *trans*-$(CH)_x$. Parallel studies of the optical properties during electrochemical isomerization will be reported elsewhere.[19] We simply note here that *cis*-to-*trans* isomerization can be conveniently accomplished by taking a $(CH)_x$ film through an electrochemical doping and undoping cycle from neutral to heavily (p or n) doped and then back to neutral.

III. EXPERIMENTAL RESULTS

A. Absorption coefficient of $[CH(ClO_4)_y]_x$ vs y

The absorption coefficient of undoped *trans*-polyacetylene is shown in Fig. 2. The open circles are from a film which was isomerized from *cis*- to

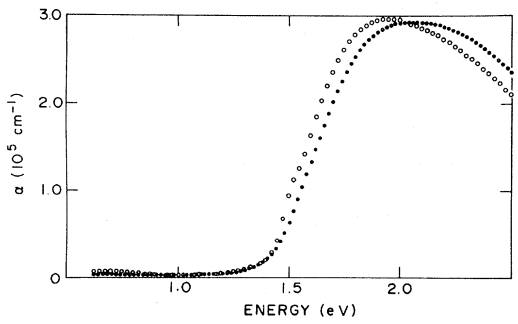

FIG. 2. Absorption coefficient of *trans*-$(CH)_x$; open circles are from a film which was thermally isomerized and closed circles are from a film which was electrochemically isomerized.

trans-$(CH)_x$ by the standard thermal isomerization procedure, whereas the solid points are from a sample which was electrochemically isomerized. The general features of the two curves are the same; however, in the case of thermal isomerization, the leading edge is steeper and the curve is more sharply peaked. The more gentle leading edge and slightly blue-shifted maximum are characteristic of electrochemical isomerization. The detailed origin of these differences is not known. We note, however, that structural studies[21] have demonstrated that thermally isomerized $(CH)_x$ films are highly crystalline with a specific interchain phase relationship. On the other hand, electrochemical isomerization involves heavy doping during which the dopant ions diffuse between the $(CH)_x$ chains. Therefore, although detailed structural data from electrochemically isomerized films are not yet available, we anticipate that the electrochemically isomerized films are probably more disordered, thus leading to the somewhat more smeared out spectral features. In this paper we deal primarily with *trans*-$(CH)_x$ films initially isomerized by means of an electrochemical cycle.

The changes indicated in Fig. 2 are not the result of chemical degradation. Subsequent electrochemical cycling of *trans*-$(CH)_x$ film can be carried out with no additional changes in the undoped *trans*-$(CH)_x$ spectrum, as shown by the two curves in Fig. 3. This is consistent with the high conductivity (indicative of high-quality material) previously reported for $[CH(ClO_4)_{0.065}]_x$ after electrochemical doping.[13] Note that the conditions under which Fig. 3 were obtained provide a rigorous test of the stability of $(CH)_x$ in the electrolyte. After taking the initial spectrum, the voltage of the cell was sequentially stepped up and then down and a series of spectra were taken over a period of about a week (see Fig. 4). As described in Sec. II, the cell utilized a thin $(CH)_x$ film (~2000-Å thickness by 2 cm^2 in area) in ~2 cm^3 of electrolyte so that the electrolyte to polymer ratio was about 10^5. Under these conditions even trace impurities in the electrolyte might lead to harmful side reactions. Nevertheless, these studies show that the $(CH)_x$ is not degraded either chemically or electrochemically during the cycle. Therefore, with moderate care in cell construction, the $(CH)_x$ electrodes can be stable in the electrochemical environment. We note, however, that we have observed irreversible degradation using cells prepared under less rigorous conditions.

Figure 4 shows a series of absorption spectra taken during the doping cycle at different applied voltages: 2.2 V ($y \simeq 0$), 3.28 V ($y=0.003$), 3.37 V ($y=0.0065$), 3.46 V ($y=0.012$), 3.57 V ($y=0.027$), 3.64 V ($y=0.047$), and 3.73 V ($y=0.078$). In each case the cell was allowed to come to diffusion equilibrium as described in Sec. II. As doping proceeds, the midgap absorption appears, centered near 0.75—0.80 eV, with an intensity which increases monotonically in proportion to the dopant concentration (see Fig. 5). The results are qualitatively nearly identical with those reported earlier for vapor-phase doping with AsF_5. Note, however, that for a given ratio of the midgap to interband peaks, the dopant concentrations determined electrochemically are about eight times higher than the estimated values quoted in the earlier work.[1]

As doping proceeds, the interband absorption peak gets progressively weaker and the corresponding oscillator strength shifts into the midgap transition. Figure 6 shows the heavily doped metallic

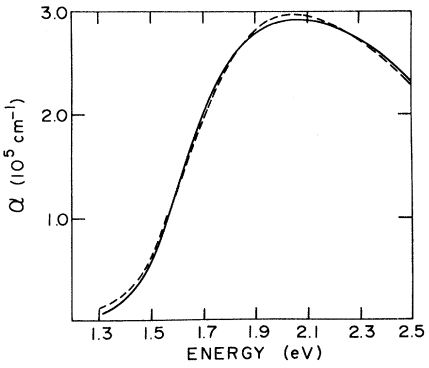

FIG. 3. Absorption coefficient of *trans*-$(CH)_x$ before (solid line) and after (dashed line) a full electrochemical doping cycle.

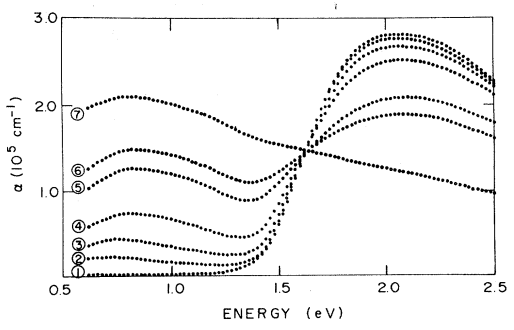

FIG. 4. Absorption spectra taken during the doping cycle at different voltage: Curve 1—2.2 V ($y=0$). Curve 2—3.28 V ($y=0.003$). Curve 3—3.37 V ($y=0.0065$). Curve 4—3.46 V ($y=0.012$). Curve 5—3.57 V ($y=0.027$). Curve 6—3.64 V ($y=0.047$). Curve 7—3.73 V ($y=0.078$).

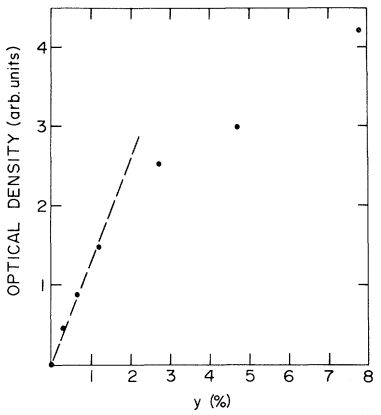

FIG. 5. Concentration dependence of the absorption coefficient at $\hbar\omega = 0.8$ eV.

case, applied voltage 3.8 V ($y \simeq 0.10$). In this case the interband transition has completely disappeared, giving rise to a free-carrier absorption. This metalliclike absorption does not appear until $y = 0.078$; at lower doping levels (see, for example, $y = 0.027$ on Fig. 4) the spectra still show a combination of midgap and interband absorptions. Even in the heavily doped regime, however, the absorption begins to decrease at long wavelengths, suggesting that the system may still show the remnants of an energy gap (or at least a minimum in the density of states).[6]

Figure 7 shows spectra from *trans*-$(CH)_x$ and from the same film after doping to $[CH(ClO_4)_y]_x$ over a photon energy range $1.6\ \text{eV} < \hbar\omega < 4\ \text{eV}$. The open circles are the data from the *trans*-$(CH)_x$ film, $\alpha_0(\omega)$, and the closed points are from the same film after dilute doping to approximately 1%, $\alpha_i(\omega)$. The solid curve was generated by multiplying $\alpha_0(\omega)$ by a constant scale factor of 0.89. The data after doping are in precise agreement with the form of Eq. (2) over the full spectral range. Taking the energy gap as $2\Delta \equiv E_g \simeq 1.5$ eV, we find that the interband absorption strength is reduced even at $\hbar\omega > 5\Delta$. Thus, the oscillator strength which appears in the midgap transition does not come from a narrow spectral range near the onset of the interband transition; it comes from the interband transition over the unusually broad spectral range predicted by Eq. (2).

B. Kinetics of electrochemical doping: The approach to equilibrium

The data of Fig. 4 were taken successively; a spectrum was taken and then the voltage was

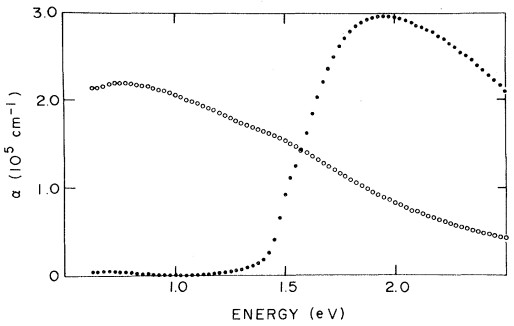

FIG. 6. Absorption spectrum from the heavily doped metallic case; 3.8 V ($y \simeq 0.1$). The curve from the same film before doping is shown for comparison.

stepped up to a new value. After allowing the cell to come to equilibrium, another spectrum was taken, etc. During the approach to diffusion equilibrium of the ClO_4^- ions, the monochrometer was set at 0.8 eV, and the strength of the midgap transition was monitored as a function of time along with the cell current $i_c(t)$. Figure 8 shows the resulting time dependence of $\delta\alpha$ (0.8 eV) and i_c on semilog plots (after stepping from 3.38 to 3.33 V on discharging). The results indicate that after an initial transient, both $\delta\alpha$ and i_c decay exponentially; e.g.,

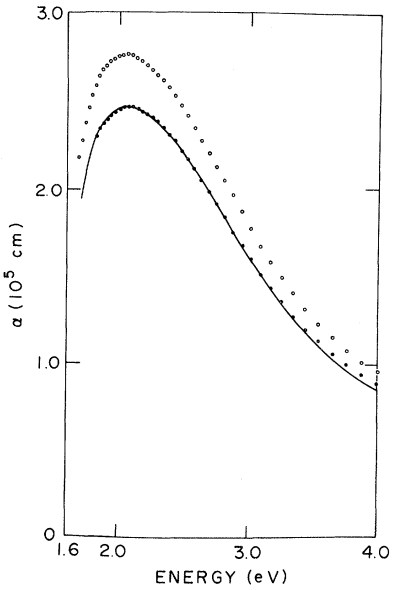

FIG. 7. Absorption coefficient over the photon energy range $1.6\ \text{eV} < \hbar\omega < 4\ \text{eV}$. Open circles are from a *trans*-$(CH)_x$ film; closed points are from the same film after doping to $[CH(ClO_4)_y]_x$ with $y \simeq 0.01$. The solid curve was generated by multiplying the initial *trans*-$(CH)_x$ data by a constant scale factor (0.89); see Eq. (2).

$$i_c(t)=i_0\exp(-t/\tau)$$

and

$$\delta\alpha\equiv(\alpha_f-\alpha_i)=\delta\alpha_0\exp(-t/\tau)\ ,$$

where α_f and α_i are final and initial values. Although there is some inaccuracy in the precise values of the decay constants (the large error bars at long time result from baseline uncertainties), the characteristic decay times for i_c and $\delta\alpha$ are consistent with one another and have magnitudes of about 10 h. Similar analyses of data at other points in the charge-discharge cycle give values for τ ranging from about 6 to 10 h.

Since the highly conducting electrolyte penetrates right into the porous $(CH)_x$ film, the establishment of a quasiequilibrium between polymer and electrolyte must take place in a relatively short time scale. The long-time changes with equilibrium values being only approximately established after many hours must, therefore, be the result of solid-state diffusion; i.e., diffusion of the dopant ions within the $(CH)_x$ fibrils. Independent electrochemical studies have also indicated that intrafibril diffusion is a slow process involving characteristic times of many hours.[22]

The *in situ* monitoring of the diffusion-limited approach to equilibrium provides quantitative criteria for the establishment of equilibrium. Since the electrolyte is in contact with the surfaces of the individual fibrils, these surfaces are initially doped more highly than the interiors after a step increase in voltage (a greater charge is placed on the surface). The experimental results show that subsequently the dopant ions redistribute throughout the bulk of the fibril in a time of order several hours (for film prepared under the conditions described in this study). The very fact that the long-time redistribution occurs at all demonstrates that it is not energetically favorable for doped *trans*-$(CH)_x$ to separate into a two-phase system, highly doped and undoped. If this were the case, then the nonuniform profile (heavily doped on the outside of a fibril and undoped at the center) would be the stable state and there would be no long-time redistribution to a more uniform configuration. That diffusion toward a uniform doping profile takes place has been independently demonstrated[23] in a study of the time evolution of the ESR signal subsequent to rapid chemical doping with Na. On a time scale of order 1 h, the observed spectrum evolves from a superposition of two lines characteristic of heavily and lightly doped regions, to a single line characteristic of a uniform concentration.

The intensity of the midgap transition shows hysteresis on the charging and discharging parts of the cycle as shown in Fig. 9. The hysteresis is large (at 3.4 V the transmitted light is an order of magnitude larger on doping than undoping) and does not result from measurements away from diffusion equilibrium, since the data points were taken after the establishment of equilibrium as described above. As a check, we include an indication of what occurs during the approach to equilibrium in the doping and undoping parts of the cycle. The data point marked 1 at 3.56 V was taken $1\frac{3}{4}$ h after the step-up from the previous point. The cell was then allowed to sit under applied voltage for approximately 17 h during which time the voltage and α evolved from 1 to 2 as shown by the arrow. Similarly the point marked 3 was taken 1 h

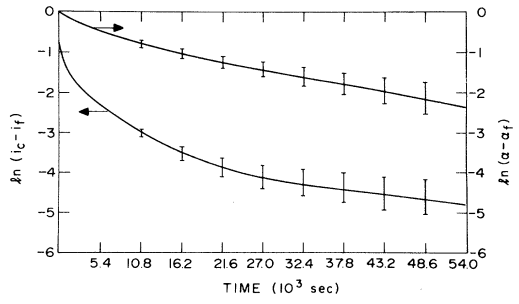

FIG. 8. Time dependence of the absorption coefficient at 0.8 eV, α, and the cell current i_c, after a step increase in applied cell voltage.

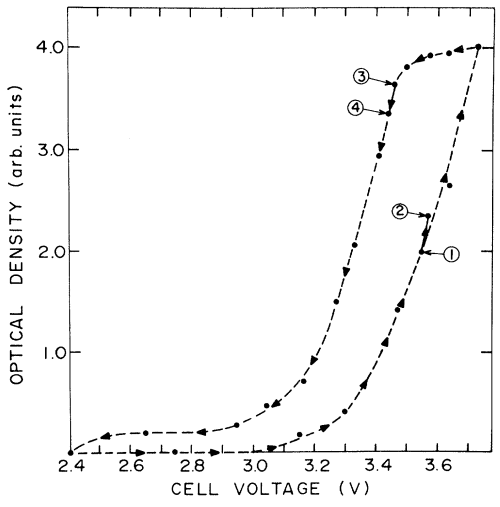

FIG. 9. The intensity of the midgap absorption α (0.8 eV), during the electrochemical cycle. Hysteresis is observed on the charging and discharging parts of the cycle (see text).

after the previous step. Again, after 16 h 3 evolved to 4. Thus the flow toward diffusion equilibrium appears to be principally along the curve defining the hysteresis.

IV. DISCUSSION

The *in situ* optical studies during electrochemical doping provide detailed quantitative information on the doping process and on the electronic structure of *trans*-$(CH)_x$ before, during, and after doping and/or undoping. Moreover, correlation of the data with transport and magnetic properties over the same dopant range can help to provide a deeper understanding of the semiconductor-metal transition.

A. The midgap transition: Solitons in *trans*-$(CH)_x$

At dilute doping levels, the results are in agreement with the predictions of the soliton model as outlined in the Introduction. The midgap transition is observed with intensity proportional to the dopant concentration (Fig. 5). In the soliton model, the absorption at dilute doping levels should be a superposition of the reduced interband transition [see Eq. (2) and Fig. 7] and the midgap transition Eq. (1). This is verified in more detail in Fig. 10. To obtain the data in Fig. 10, the interband absorption was subtracted from the data for 0.65% doping, using a scale factor such that the doped and undoped curves agree at frequencies

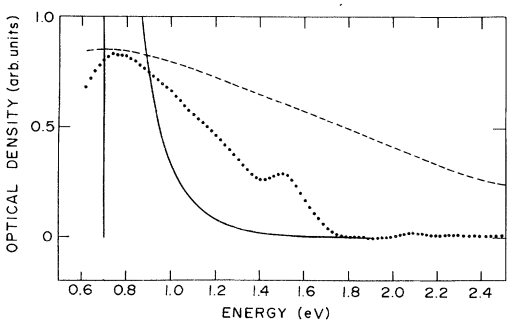

FIG. 10. Midgap transition for $y=0.0065$; the interband absorption was subtracted using a scale factor such that the doped and undoped curves agree at high frequencies (see Fig. 7). The theoretical curve, Eq. (1), is superposed for comparison (solid). The dashed curve is the free-carrier data from heavily doped metallic $(CH)_x$ (see Fig. 6).

well above the gap (see Fig. 7). The theoretical curve [Eq. (1)] is superposed for comparison. Although the singularity at $\hbar\omega=\frac{1}{2}E_g$ is rounded, the characteristic asymmetric line shape described by Eq. (1) is in general agreement with the data. The square-root singularity is expected to be smeared out by a combination of disorder and the effects of interchain coupling. Such effects are also important in determining the shape of the interband absorption. However, the sech^2 factor in Eq. (1) tends to make the midgap absorption fall off more rapidly than the interband transition with increasing energy. This is evident in the data, both in the width and the peak position; the peak of the midgap absorption is shifted less than that of the interband transition (by disorder, etc.) from the ideal value. Thus, to the accuracy of our measurements, the intense near-infrared absorption (centered near 0.75 eV), which appears on doping, implies the existence of a relatively narrow localized level within about 0.1 eV of the gap center.

The second prediction of the soliton calculation is expressed in Eq. (2). In the presence of a soliton, the interband absorption should be uniformly decreased, so that the total oscillator strength is conserved. It is clear from Figs. 4 and 7 that the interband transition is reduced over an unusually wide range. As shown in Fig. 7, the decrease is as given in Eq. (2); i.e., a uniform dilution with no change in shape. Quantitative comparison of the reduction in interband intensity with theory can be used to obtain the prefactor $[1-2(\xi/a)y]$ in Eq. (2). Using the data from Figs. 4 and 7 one estimates $\xi/a\simeq 6\pm 2$ in excellent agreement with the parameters of the SSH model. For $y\simeq 0.01$, the integrated absorption associated with the midgap transition is about 12% of the original interband transition, and the interband strength is reduced by a comparable amount (Fig. 7). The quantitative results for several dilute concentrations are summarized in Table I. Thus, to within the error, the integrated oscillator strength is conserved and Eqs. (1) and (2) are valid.

Using Eqs. (1) and (2), the absorption coefficient can be written as

$$\alpha(\omega)=f\alpha_s'(\omega)+(1-f)\alpha_0(\omega)\ , \tag{4}$$

where $f=2(\xi/a)y$, $\alpha_0(\omega)$ is the interband transition in absence of doping [i.e., Eq. (3)], and

$$\alpha_s(\omega)=(2\xi/a)\alpha_s'(\omega)\ , \tag{5}$$

TABLE I. Comparison of midgap and interband oscillator strengths.

y	Fractional gain at midgap $\int \alpha_s(\omega)d\omega / \int \alpha_0(\omega)d\omega$	Loss from interband transition[a] $\left[1-\frac{2\xi}{a}y\right]_{\text{exp}}$
0.003	0.025	0.020
0.0065	0.053	0.050
0.012	0.120	0.110

[a]Note that $[1-(2\xi/a)y]=\alpha_i(\omega)/\alpha_0(\omega)\simeq \int \alpha_i(\omega)d\omega / \int \alpha_0(\omega)d\omega$.

with $\alpha_s(\omega)$ given in Eq. (1). This expression is valid both in the dilute regime and at intermediate levels where a soliton lattice is expected to form.[24] The structure of Eq. (4) implies that there should be an isosbestic point in the absorption curves. This point is clearly evident at $\hbar\omega=1.63$ eV in the data plotted on Fig. 4. Similarly, an isosobestic point is observed for the undoping part of the cycle (discharge) at a slightly lower photon energy (1.57 eV).

B. The metallic "particles" model

Tomkiewicz *et al.*[25] and Wegner[26] have argued that the doping of $(CH)_x$ is intrinsically inhomogenous and leads to the formation of metallic "islands." In their view, the semiconductor-metal transition is a percolation transition at which point a connected metallic path first appears. We have shown, however, that the combination of transport and magnetic data rule out such a percolation transition.[27–29] Moreover, as demonstrated in Sec. III, the long-time diffusion observed in the kinetic studies reported in this paper indicate that a two-phase separation into heavily doped (metallic) and undoped (or lightly doped) regions is not energetically favorable in *trans*-$(CH)_x$. Direct confirming evidence against the formation of metallic "particles" can be found in the optical data. In the metallic particle view, small regions are metallic well below the percolation transition. If this were the case, the absorption would be a superposition of the free-carrier absorption (cut off at long wavelengths by particle depolarization effects) and the undoped interband transition. The assumed superposition of the free-carrier absorption (Fig. 6) and the interband transition is tested in Fig. 10. The free-carrier curve from heavily doped metallic *trans*-$(CH)_x$ (Fig. 6) is superposed for comparision with the data from dilute doping. The differences are apparent; the absorption data at dilute doping levels are not consistent with the formation of small metallic particles.

C. Identification of carriers in the transitional regime

Throughout the intermediate doping regime, $0.002<y<0.05$, the optical studies show the simultaneous existence of the midgap transition and the interband transition. This is particularly important in the context of transport and magnetic studies of the transitional regime. The thermopower and electrical conductivity[27] imply a transition at a concentration of about $y\simeq 0.001$, whereas the Pauli susceptibility[28] (and hence the density of states) remains small until concentrations in excess of $y\simeq 0.05$. The absence of Pauli susceptibility until $y>0.07$ is consistent with the optical data; only for

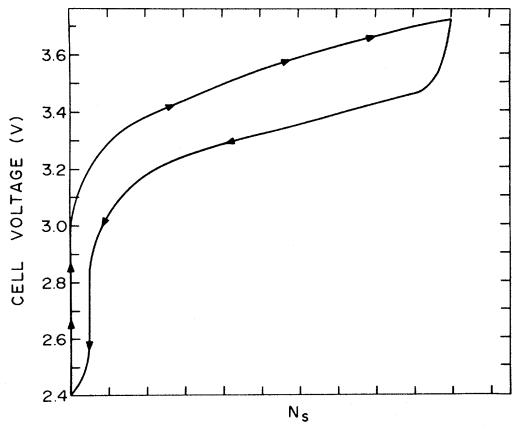

FIG. 11. Number of solitons N_s as a function of cell voltage. The curves are obtained from Fig. 9, assuming a linear relation between the 0.8-eV absorption and the number of solitons (see text).

$y=0.078$ does the interband transition completely disappear giving rise to a free-carrier absorption.

An important feature of the transition from the dilute regime, characterized by Kivelson's intersoliton hopping,[29] to the highly conducting nonmagnetic regime[28] is demonstrated in the thermopower data. The small values and quasilinear (with temperature) behavior observed for $y > 0.002$ imply delocalized carrier transport. However, these carriers cannot arise from simple band states. The optical data presented in this paper identify the carriers in this regime: Since the midgap transition is clearly evident, the carriers responsible for the high conductivity in the transitional regime are solitons. Thus a generalized soliton picture, involving delocalized carriers, appears to be implied by the combination of optical, magnetic, and transport data.

D. Hysteresis: Charge injection via polarons; charge removal via solitons

The hysteresis in the strength of the midgap absorption is unusual. Since the absorption at 0.8 eV is proportional to the soliton (and dopant) concentration, the observed hysteresis implies that charge is injected at higher voltages and taken out at lower voltages when the system is close to diffusion equilibrium. This is emphasized in Fig. 11 where we plot the number of solitons N_s as a function of cell voltage. Figure 11 is schematic and assumes a linear relation between the 0.8-eV absorption coefficient and the number of solitions. This appears to be valid at low doping levels with a saturation at higher levels (as shown in Fig. 5). Deviation from linearity will not qualitatively change the shape of the curves in Fig. 11. There is a threshold for charge injection near 3 V and a clear hysteresis; the injected solitions are not all removed until the voltage is reduced below about 2.5 eV. These features have also been observed in direct electrochemical studies using electrochemical voltage spectroscopy.[30]

Charge is injected in the electrochemical cell when the applied voltage is large enough to allow oxidation (p-type doping) or small enough to allow reduction (n-type doping). In a traditional semiconductor this would occur at $V_0=\frac{1}{2}E_g$, since the chemical potential of the pure semiconductor is at the center of the gap. This assumes that both the semiconductor and the electrolyte are at a constant potential and that all the voltage drop is at the semiconductor-electrolyte interface. Under these circumstances, the electrochemical cell can be used to study, in effect, electron injection into (or out of) the semiconductor in a manner analogous to a tunneling junction. Note, however, that each electronic charge injected at the electrode must be accompanied by the insertion of a dopant ion from the electrolyte to assure charge neutrality. Thus, the high surface area of fibrillar $(CH)_x$ is a critical feature. Within a rigid-band model for the semiconductor, there would be no hysteresis; charge would go in and come out at $V_0=\Delta$.

The essence of the soliton theory is that a rigid-band picture for *trans*-$(CH)_x$ is simply and fundamentally not valid. Upon injection of a charge into *trans*-$(CH)_x$, the electron-phonon coupling causes the lattice to distort leading to the formation of a polaron (single charge) or a pair of solitons (one charge for each). Since solitons can only be formed in pairs, injection of a single charge must lead to polaron formation rather than soliton formation. However, continued injection of single (positive) charges will lead to a finite density of polarons and a reaction to form the lower-energy configuration of a charged soliton-antisoliton pair:

$$p^+ + p^+ \rightarrow S^+ + \tilde{S}^+ ,$$

where p stands for polaron and S ($\tilde{S}$) for soliton (antisoliton).

The hysteresis of Figs. 10 and 11 can be understood in this manner. The key point is that single charges are injected at the interface between the polymer and the conducting glass substrate. Thus, initially polarons should be formed. The corresponding energy would be approximately the single-particle energy (charge injection followed by lattice deformation); $V_0 \simeq \Delta$. Taking $V_0^{\text{expt}} \simeq 3.0$ V and $\Delta \sim 0.7$ eV would imply that neutral *trans*-$(CH)_x$ is positive with respect to Li metal by about 2.3 V. This value is consistent with electrochemical data which typically give open-circuit voltage values in the range 2.2—2.6 V for neutral $(CH)_x$ vs Li. However, as indicated above, the polarons are energetically unstable and are expected to combine to form solitons. The midgap absorption, therefore, turns on at about 3.0 V. However, having formed the solitons, charge can be subsequently extracted from the midgap levels (since the soliton electronic levels can have charge 0 or $\pm$ 1). As the charges are withdrawn, neutral soliton pairs on a chain will quickly annihilate leaving the undoped *trans*-$(CH)_x$ chain. Since the charge is removed from the midgap state, the midgap absorption

would not disappear until the applied voltage is reduced such that the electrochemical potential is that of neutral *trans*-$(CH)_x$; i.e., about 2.2—2.6 V. The data of Figs. 10 and 11 are in full agreement with these ideas.

The hysteresis is expected to occur when the charge injection (or removal) rates are sufficiently large that the number of polarons is determined by the current. In this case, the electrochemical potential is pinned at the band edge during injection and at the midgap level during charge removal. This is the case in the experiments described above. At sufficiently low current levels and sufficiently high absolute temperatures, however, thermally excited polarons will determine the position of the chemical potential. In this limit the hysteresis would be correspondingly reduced. Preliminary electrochemical experiments (V vs Q) at much lower current levels (per unit mass of film) than used here show evidence of such behavior.[22]

The weak secondary absorption at $\hbar\omega \simeq 1.4$ eV in Fig. 10 occurs at approximately the energy expected for the optical transition between the localized states of a polaron,[31,32] $\hbar\omega = 2\Delta/\sqrt{2}$. Preliminary results suggest that this additional narrow peak may be taken as evidence of (transient) polaron formation due to single-charge injection during electrochemical doping. *In situ* studies of the 1.4-eV absorption during electrochemical doping and undoping are underway and will be reported in detail elsewhere.[33]

V. CONCLUSION

The general features of the midgap absorption induced by doping *trans*-$(CH)_x$ have now been demonstrated to be quite universal and independent of dopant species. The same spectral features (i.e., the shape and the energy) are found for a variety of p-type dopants using either chemical or electrochemical doping.[1,7] Moreover, the same absorption band is obtained after n-type chemical doping (e.g., Na^+ napthalide in solution).[8] This universality implies that the doping-induced absorption is a characteristic feature of the doped *trans*-$(CH)_x$ chain and not a donor and/or acceptor state of the type commonly found in semiconductors. In the latter case, the energy of the bound state would be sensitive to the dopant species. However, as a result of electron-hole symmetry each soliton introduces a state with energy at the center of the gap. As shown above, the observed midgap transition indicates the presence of a narrow level within 0.1 eV of the gap center. Moreover, the changes in oscillator strength are consistent with the parameters of the SSH model. We conclude that the midgap absorption observed in *trans*-$(CH)_x$ provides direct evidence for the existence of charged solitons. Moreover, the persistence of these spectral features into the transitional regime ($0.002 < y < 0.07$) identifies the dominant charge carriers in this regime as charged solitons.

Kinetic studies following a step change in applied cell voltage indicate a time constant for the approach to equilibrium (after an initial faster transient) of several hours, apparently limited by relatively slow solid-state diffusion of the dopant ions within the $(CH)_x$ fibrils. That this long-time redistribution occurs demonstrates that it is not energetically favorable for the doped *trans*-$(CH)_x$ to separate into a two-phase system, i.e., metallic "islands." If this were the case, then the nonuniform profile obtained after a step change in applied voltage (heavily doped on the outside of a fibril and undoped at the center) would be the stable state and there would be no long-time redistribution to a more uniform configuration. Direct confirming evidence against metallic particle formation has been obtained from the spectroscopic data; the midgap absorption at dilute doping is not consistent with the free-carrier absorption observed in the metallic regime.

The hysteresis in the intensity of the midgap absorption as a function of applied voltage (on charge and discharge) has been interpreted as a direct indication of single-charge injection via polarons which subsequently combine to form charged soliton pairs. These observations open a new opportunity for studies of the electronic structure of conducting polymers. Much remains to be clarified in this area. For example, we suggested that the charge-injection energy was the single-particle energy (Δ) rather than the polaron formation energy (E_p) based on the argument that charge is first injected and then the distortion occurs. However, since the injection takes place at quasiequilibrium, one might equally argue that injection should occur at $E_p = 2\sqrt{2}\Delta/\pi$. Since numerically $E_p \simeq 0.9\Delta$, careful work at relatively high resolution will be required to resolve the question. It is evident, however, that such *in situ* opto-electrochemical techniques provide a powerful and elegant experimental probe which is perhaps uniquely suited to the study of doping in conducting polymers.

ACKNOWLEDGMENT

This study was supported in part by the Office of Naval Research/Defense Advanced Research Projects Agency (ONR/DARPA) and in part by the Department of Energy (DOE) (Advanced Energy projects; DE-AC02-81ER-10832). The optical measurements were supported by ONR/DARPA; the fabrication, characterization, and evaluation of stable cells used in the measurements was supported by the DOE. We thank Dr. K. Kaneto for many useful discussions.

[1]N. Suzuki, M. Ozaki, S. Etemad, A. J. Heeger, and A. G. MacDiarmid, Phys. Rev. Lett. 45, 1209 (1980).
[2]W. P. Su, J. R. Schrieffer, and A. J. Heeger, Phys. Rev. Lett. 42, 1698 (1979).
[3]W. P. Su, J. R. Schrieffer, and A. J. Heeger, Phys. Rev. Lett. B 22, 2099 (1980).
[4]M. J. Rice, Phys. Lett. 71A, 152 (1979).
[5]H. Takayama, Y. R. Lin-Liu, and K. Maki, Phys. Rev. B 21, 2388 (1980).
[6]E. J. Mele and M. J. Rice, Phys. Rev. B 23, 5397 (1981).
[7]M. Tanaka, A. Watanabe, and J. Tanaka, Bull. Chem. Soc. Jpn. 53, 645 (1980); 53, 3430 (1980).
[8]T.-C. Chung, A. Feldblum, A. J. Heeger, and A. G. MacDiarmid, J. Chem. Phys. 74, 5504 (1981).
[9]J. T. Gammel and J. A. Krumhansl, Phys. Rev. B 24, 1035 (1981), and report (unpublished).
[10]S. Kivelson, T. K. Lee, Y. R. Lin-Liu, I. Peschel, and Lu Yu, Phys. Rev. B 6, 4173 (1982).
[11]K. Maki and M. Nakahara, Phys. Rev. B 23, 5005 (1981).
[12]N. Suzuki, M. Ozaki, S. Etemad, A. J. Heeger, and A. G. MacDiarmid, Phys. Rev. Lett. 45, 1463 (1980).
[13]P. J. Nigrey, A. G. MacDiarmid, and A. J. Heeger, J. Chem. Soc. Chem. Commun. 1979, 594.
[14]D. MacInnes, Jr., M. A. Druy, A. J. Nigrey, D. P. Nairns, A. G. MacDiarmid, and A. J. Heeger, J. Chem. Soc. Chem. Commun. 1981, 317.
[15]P. J. Nigrey, D. MacInnes, Jr. D. P. Nairns, A. G. MacDiarmid, and A. J. Heeger, J. Electrochem. Soc. 128, 1651 (1981).
[16]K. Kaneto, T.-C. Chung, R. Kaner, J. Kaufman, A. G. MacDiarmid, and A. J. Heeger (unpublished).
[17]H. Shirakawa and S. Ikeda, Polym. J. 2, 231 (1971); H. Shirakawa, T. Ito, and S. Ikeda, *ibid.* 4, 460 (1973); T. Ito, H. Shirakawa, and S. Ikeda, J. Polym. Sci. Polym. Chem. Ed. 12, 11 (1974); 13, 1943 (1975); H. Shirakawa, T. Ito, and S. Ikeda, Die Macromol. Chem. 179, 1565 (1978).
[18]T.-C. Chung, Ph.D. thesis, University of Pennsylvania, 1982 (unpublished).
[19]T.-C. Chung, A. Feldblum, A. G. MacDiarmid, and A. J. Heeger, J. Polym. Sci. Polym. Lett. Ed. (in press).
[20]T. C. Clarke and J. C. Scott (unpublished).
[21]C. R. Fincher, Jr., C.-G. Chen, A. J. Heeger, A. G. MacDiarmid, and J. B. Hastings, Phys. Rev. Lett. 48, 100 (1982).
[22]K. Kaneto, A. G. MacDiarmid, and A. J. Heeger (unpublished).
[23]J. J. Andre (unpublished).
[24]B. Horovitz, Solid State Commun. 41, 729 (1982).
[25]Y. Tomkiewicz, T. D. Schultz, H. B. Brom, T. C. Clarke, and G. B. Street, Phys. Rev. Lett. 43, 1532 (1979); Y. Tomkiewicz, T. D. Schultz, H. B. Brom, A. R. Taranko, T. C. Clarke, and G. B. Street, Phys. Rev. B 24, 4348 (1981).
[26]G. Wegner, Angew. Chem. Int. Ed. Engl. 20, 361 (1981).
[27]D. Moses, A. Denenstein, J. Chen, P. McAndrew, T. Woerner, A. J. Heeger, A. G. MacDiarmid, and Y. W. Park, Phys. Rev. B 25, 7652 (1982).
[28]S. Ikehata, J. Kaufer, T. Woerner, A. Pron, M. A. Druy, A. Sivak, A. J. Heeger, and A. G. MacDiarmid, Phys. Rev. Lett. 45, 1123 (1980); see also A. J. Epstein, H. Rommelmann, M. A. Druy, A. J. Heeger, and A. G. MacDiarmid, Solid State Commun. 38, 683 (1981); J. Flood, S. Iketa, T. Woerner, M. A. Druy, A. J. Heeger, and A. G. MacDiarmid (unpublished).
[29]S. Kivelson, Phys. Rev. Lett. 46, 1344 (1981).
[30]J. Kaufman, A. Kaner, A. J. Heeger, and A. G. MacDiarmid (unpublished).
[31]D. Campbell and A. R. Bishop, Phys. Rev. B 24, 4859 (1981).
[32]S. Brazovskii and N. Kirova, Pis'ma Zh. Eksp. Teor. Fiz. 33, 8 (1981).
[33]A. Feldblum, S. Etemad, A. J. Heeger, T.-C. Chung, and A. G. MacDiarmid (unpublished).